

# UCLA

## UCLA Previously Published Works

### Title

Mice expressing fluorescent PAR2 reveal that endocytosis mediates colonic inflammation and pain

### Permalink

<https://escholarship.org/uc/item/7sz693hs>

### Journal

Proceedings of the National Academy of Sciences of the United States of America, 119(6)

### ISSN

0027-8424

### Authors

Latorre, Rocco  
Hegron, Alan  
Peach, Chloe J  
[et al.](#)

### Publication Date

2022-02-08

### DOI

10.1073/pnas.2112059119

### Copyright Information

This work is made available under the terms of a Creative Commons Attribution-NonCommercial-NoDerivatives License, available at <https://creativecommons.org/licenses/by-nc-nd/4.0/>

Peer reviewed



# Mice expressing fluorescent PAR<sub>2</sub> reveal that endocytosis mediates colonic inflammation and pain

Rocco Latorre<sup>a,b</sup>, Alan Hegron<sup>a,b</sup>, Chloe J. Peach<sup>a,b</sup>, Shavonne Teng<sup>a,b</sup>, Raquel Tonello<sup>a,b</sup>, Jeffri S. Retamal<sup>a,b,c</sup>, Rafael Klein-Cloud<sup>a,b</sup>, Diana Bok<sup>a,b,c</sup>, Dane D. Jensen<sup>a,b,c</sup>, Lena Gottesman-Katz<sup>a,b</sup>, Jeanette Rientjes<sup>d</sup>, Nicholas A. Veldhuis<sup>e</sup>, Daniel P. Poole<sup>e</sup>, Brian L. Schmidt<sup>a,b,c</sup>, Charalabos H. Pothoulakis<sup>f</sup>, Carl Rankin<sup>f</sup>, Ying Xie<sup>f</sup>, Hon Wai Koon<sup>f</sup>, and Nigel W. Bunnett<sup>a,b,1</sup>

<sup>a</sup>Department of Molecular Pathobiology, Neuroscience Institute, New York University, New York, NY 10010; <sup>b</sup>Department of Neuroscience and Physiology, Neuroscience Institute, New York University, New York, NY 10010; <sup>c</sup>Bluestone Center for Clinical Research, New York University College of Dentistry, New York, NY 10010; <sup>d</sup>Gene Modification Platform, Monash University, Clayton, VIC 3168, Australia; <sup>e</sup>Drug Discovery Biology, Monash Institute of Pharmaceutical Sciences, Monash University, Parkville, VIC 3052, Australia; and <sup>f</sup>Vatche and Tamar Manoukian Division of Digestive Diseases, David Geffen School of Medicine, University of California, Los Angeles, CA 90095

Edited by Robert Lefkowitz, Medicine and Biochemistry, Howard Hughes Medical Institute, Durham, NC; received June 30, 2021; accepted December 22, 2021

**G protein-coupled receptors (GPCRs) regulate many pathophysiological processes and are major therapeutic targets. The impact of disease on the subcellular distribution and function of GPCRs is poorly understood. We investigated trafficking and signaling of protease-activated receptor 2 (PAR<sub>2</sub>) in colitis. To localize PAR<sub>2</sub> and assess redistribution during disease, we generated knockin mice expressing PAR<sub>2</sub> fused to monomeric ultrastable green fluorescent protein (muGFP). PAR<sub>2</sub>-muGFP signaled and trafficked normally. PAR<sub>2</sub> messenger RNA was detected at similar levels in *Par<sub>2</sub>-muGFP* and wild-type mice. Immunostaining with a GFP antibody and RNAScope in situ hybridization using *F2rl1* (PAR<sub>2</sub>) and *Gfp* probes revealed that PAR<sub>2</sub>-muGFP was expressed in epithelial cells of the small and large intestine and in subsets of enteric and dorsal root ganglia neurons. In healthy mice, PAR<sub>2</sub>-muGFP was prominently localized to the basolateral membrane of colonocytes. In mice with colitis, PAR<sub>2</sub>-muGFP was depleted from the plasma membrane of colonocytes and redistributed to early endosomes, consistent with generation of proinflammatory proteases that activate PAR<sub>2</sub>. PAR<sub>2</sub> agonists stimulated endocytosis of PAR<sub>2</sub> and recruitment of Gα<sub>q</sub>, Gα<sub>i</sub>, and β-arrestin to early endosomes of T84 colon carcinoma cells. PAR<sub>2</sub> agonists increased paracellular permeability of colonic epithelial cells, induced colonic inflammation and hyperalgesia in mice, and stimulated proinflammatory cytokine release from segments of human colon. Knockdown of dynamin-2 (*Dnm2*), the major colonocyte isoform, and Dnm inhibition attenuated PAR<sub>2</sub> endocytosis, signaling complex assembly and colonic inflammation and hyperalgesia. Thus, PAR<sub>2</sub> endocytosis sustains protease-evoked inflammation and nociception and PAR<sub>2</sub> in endosomes is a potential therapeutic target for colitis.**

signaling | receptors | proteases | endocytosis | inflammation

**G** protein-coupled receptors (GPCRs) are the largest family of transmembrane receptors, control most physiological and pathological processes, and are the target of >30% of approved drugs (1). Despite their medical importance, the effects of disease on the function and subcellular distribution of GPCRs are poorly understood. GPCRs at the plasma membrane interact with extracellular ligands and couple to intracellular heterotrimeric G proteins. However, GPCR signaling at the plasma membrane is often transient. GPCR kinases phosphorylate activated receptors, increasing their affinity for β-arrestins (βARRs) (2). βARRs uncouple GPCRs from G proteins, which mediates desensitization, and couple GPCRs to clathrin and adaptor protein 2, which mediate endocytosis. These processes terminate plasma membrane signaling. During disease, the continued generation of agonists could trigger the endocytosis of GPCRs. Although endosomes were once considered merely as a pathway for receptor trafficking, mounting evidence indicates that endosomes are a site of sustained GPCR

signaling by Gα- and βARR-mediated mechanisms (3–9). GPCRs can also continue to signal from other intracellular compartments, including the Golgi apparatus (10, 11). The contribution of intracellular GPCR signaling to disease is not fully understood.

We investigated the impact of colitis on endosomal signaling of protease-activated receptor 2 (PAR<sub>2</sub>), which mediates the proinflammatory and pronociceptive actions of proteases (12). Trypsin (13), tryptase (14), coagulation factors VIIa and Xa (15), and kallikreins (16) cleave PAR<sub>2</sub> to reveal a tethered ligand that activates the receptor. Cathepsin S, legumain, and elastase cleave at different sites and activate biased mechanisms of PAR<sub>2</sub> signaling (17–19). During colitis, multiple proteases from the host and the microbiome activate PAR<sub>2</sub> (20–25). PAR<sub>2</sub> activation evokes the redistribution of ZO1 and occludin

## Significance

**Colonic epithelial cells protect against inflammation by forming a barrier against ingress of microbes, digestive enzymes, and metabolic waste from the lumen. Protease-activated receptor-2 (PAR<sub>2</sub>) mediates the proinflammatory and pronociceptive actions of proteases. We found that the proteolytic environment of the inflamed mouse colon induces redistribution of PAR<sub>2</sub> from the basolateral plasma membrane to endosomes of colonocytes. Endocytosis allows the assembly of a PAR<sub>2</sub>, Gα, and β-arrestin signaling complex that mediates sustained increases in colonocyte paracellular permeability and persistent inflammation and hyperalgesia of the colon. Thus, PAR<sub>2</sub> endocytosis and endosomal signaling disrupts the normal protective function of colonocytes and underlies colonic inflammation and pain. PAR<sub>2</sub> in endosomes is a potential therapeutic target for inflammatory and painful diseases of the colon.**

Author contributions: R.L., A.H., C.J.P., R.T., J.S.R., R.K.-C., D.D.J., J.R., N.A.V., D.P.P., C.H.P., Y.X., H.W.K., and N.W.B. designed research; R.L., A.H., C.J.P., S.L.T., R.T., J.S.R., R.K.-C., D.B., D.D.J., L.G.-K., J.R., N.A.V., D.P.P., C.R.R., Y.X., and H.W.K. performed research; J.R., C.H.P., Y.X., and H.W.K. contributed new reagents/analytic tools; R.L., A.H., C.J.P., S.L.T., R.T., J.S.R., R.K.-C., D.D.J., L.G.-K., J.R., N.A.V., D.P.P., B.L.S., C.R.R., Y.X., H.W.K., and N.W.B. analyzed data; and R.L., A.H., C.J.P., R.T., J.S.R., D.D.J., N.A.V., D.P.P., B.L.S., H.W.K., and N.W.B. wrote the paper.

Competing interest statement: N.W.B. is a founding scientist of Endosome Therapeutics, Inc. Research in the laboratories of N.W.B., N.A.V., and D.P.P. is funded in part by Takeda Pharmaceuticals International.

This article is a PNAS Direct Submission.

This article is distributed under [Creative Commons Attribution-NonCommercial-NoDerivatives License 4.0 \(CC BY-NC-ND\)](https://creativecommons.org/licenses/by-nc-nd/4.0/).

<sup>1</sup>To whom correspondence may be addressed. Email: nwb2@nyu.edu.

This article contains supporting information online at <http://www.pnas.org/lookup/suppl/doi:10.1073/pnas.2112059119/-DCSupplemental>.

Published February 2, 2022.

from tight junctions of colonocytes, leading to increased paracellular permeability, influx of proinflammatory macromolecules and bacteria into the mucosa, and inflammation (26, 27). PAR<sub>2</sub> activation on nociceptors stimulates the release of neuropeptides that cause neurogenic inflammation and pain in the skin (28, 29) and colon (7, 22, 30). Proteases and PAR<sub>2</sub> have been implicated in colonic diseases, including inflammatory bowel disease (IBD), irritable bowel syndrome, and cancer (12). However, the signaling mechanisms by which PAR<sub>2</sub> induces disease are incompletely understood.

Our understanding of the function of PAR<sub>2</sub> is hampered by an inadequate knowledge of its cellular and subcellular localization in health and disease states. Because GPCR antibodies can lack sensitivity and specificity and are unsuitable for studying receptor trafficking in living cells, we generated a knockin mouse expressing PAR<sub>2</sub> fused to monomeric ultrastable green fluorescent protein (muGFP). Colitis resulted in translocation of PAR<sub>2</sub>-muGFP from the basolateral membrane of colonocytes to early endosomes. Endocytosis of PAR<sub>2</sub> led to the assembly of a signaling complex (signalosome) comprising PAR<sub>2</sub> and Gα<sub>q</sub>, Gα<sub>i</sub>, or βARR. Endocytosis of PAR<sub>2</sub> was necessary for sustained increases in paracellular permeability, release of proinflammatory cytokines and chemokines, and colonic inflammation and hyperalgesia.

## Results

**Generation of *Par<sub>2</sub>-mugfp* Mice.** To gain an understanding of the cellular and subcellular distribution of PAR<sub>2</sub> and how it might be altered during disease, we generated mice expressing mouse PAR<sub>2</sub> fused at the intracellular C terminus to muGFP. muGFP harbors stabilizing mutations (Q69L and N164Y), which improve hydrophobic packing in the core and facilitate hydrogen bonding, and a mutation at the dimer interface (F223D), which prevents dimerization (31). muGFP retains fluorescence after harsh fixation and resists undesirable dimerization. To verify functionality of PAR<sub>2</sub>-muGFP, we compared signaling of PAR<sub>2</sub>-muGFP and PAR<sub>2</sub> with N-terminal FLAG and C-terminal HA11 epitopes transiently expressed in KNRK cells, which express low levels of PAR<sub>2</sub> and have been used extensively to study PAR<sub>2</sub> functions (13). Trypsin and 2-furoyl-LIGRLO-NH<sub>2</sub> (2F), a PAR<sub>2</sub> agonist that is an analog of the tethered ligand domain, stimulated a concentration-dependent increase in IP-1 formation with similar potency and efficacy in cells expressing PAR<sub>2</sub>-muGFP or PAR<sub>2</sub>-HA11 (half maximal effective concentration of KNRK-PAR<sub>2</sub>-muGFP: trypsin, 5.4 × 10<sup>8</sup> M; 2F, 9.1 × 10<sup>8</sup> M; half maximal effective concentration of KNRK-PAR<sub>2</sub>-HA11: trypsin, 5.4 × 10<sup>8</sup> M; 2F, 7.8 × 10<sup>8</sup> M) (*SI Appendix, Fig. S1 A and B*). There were no responses to trypsin or 2F in cells expressing muGFP alone. Thus, PAR<sub>2</sub>-muGFP signals similarly to PAR<sub>2</sub>-HA11 in KNRK cells, suggesting that muGFP does not affect the normal functions of PAR<sub>2</sub>.

To generate knockin mice, a targeting construct was generated comprising *Par<sub>2</sub>-mugfp*, a floxed PGK neomycin cassette, and a downstream KpnI site for Southern screening (Fig. 1A). Five embryonic stem cell clones expressing the construct were identified by Southern blotting (1.25% incorporation); blotting at the 3' and 5' arms of homology confirmed correct targeting (Fig. 1B). Screening with an internal probe to the NEO cassette excluded random integration or insertion of a concatemer. The presence and the integrity of *loxP* sites and insertion of *Par<sub>2</sub>-mugfp* were verified by sequencing. Two clones were injected into BALB/c mouse blastocysts. Chimeras (black and white) were generated from both clones and bred with wild-type C57BL6J female mice to generate black F1 progeny, indicating germline transmission. Expression of *Par<sub>2</sub>-mugfp* was confirmed by Southern blotting (Fig. 1C) and reverse-transcription polymerase chain reaction (RT-PCR) (Fig. 1D).

**Characterization of *Par<sub>2</sub>-mugfp* Mice.** We compared the expression of *F2rl1*, the gene encoding for PAR<sub>2</sub>, in *Par<sub>2</sub>-mugfp* and wild-type mice using quantitative RT-PCR (qRT-PCR). *F2rl1* expression in the stomach, duodenum, ileum, colon, and dorsal root ganglia (DRG) was not different in *Par<sub>2</sub>-mugfp* and wild-type mice (Fig. 1E). *F2rl1* was expressed at higher levels in the jejunum of *Par<sub>2</sub>-mugfp* mice for unknown reasons. Thus, in most tissues, *F2rl1* is expressed at similar levels in *Par<sub>2</sub>-mugfp* and wild-type mice.

## Localization of PAR<sub>2</sub>-muGFP Immunoreactivity and Messenger RNA.

We localized PAR<sub>2</sub>-muGFP by indirect immunofluorescence and confocal microscopy using a GFP antibody to amplify the signal. This approach avoided use of GPCR antibodies, which can lack selectivity. In *Par<sub>2</sub>-mugfp* mice, GFP immunoreactivity was prominently localized to the basolateral plasma membrane of epithelial cells of the villi and crypts in the duodenum, jejunum, ileum, and lining mucosal folds and crypts in the colon (Fig. 2A and B). There was no detectable GFP immunoreactivity in epithelial cells of the small or large intestine of wild-type mice, which confirms selectivity of the GFP antibody (Fig. 2A and B). PAR<sub>2</sub>-muGFP immunoreactivity was detected at low levels in the enteric nervous system of the small and large intestines of *Par<sub>2</sub>-mugfp* mice, but the cellular localization was not further studied.

We used RNAScope in situ hybridization with probes to *F2rl1* and *Gfp* to confirm PAR<sub>2</sub>-muGFP localization in the colon. In *Par<sub>2</sub>-mugfp* mice, *F2rl1* and *Gfp* were prominently detected in colonocytes (Fig. 2C). In wild-type mice, *F2rl1*, but not *Gfp*, was detected in colonocytes. RNAScope was used to detect PAR<sub>2</sub> expression with high sensitivity in DRG neurons. In *Par<sub>2</sub>-mugfp* mice, *F2rl1*, and *Gfp* were coexpressed in a subpopulation of DRG neurons (Fig. 2D). *F2rl1*, but not *Gfp*, was expressed in DRG neurons of wild-type mice (Fig. 2E).

These results confirm the expression of PAR<sub>2</sub> in intestinal epithelial cells and a subpopulation of primary sensory neurons, and they validate the use of *Par<sub>2</sub>-mugfp* mice for studies of the cellular localization of this receptor.

**Agonist-Evoked Trafficking of PAR<sub>2</sub>-muGFP in the Colon.** Upon activation, many GPCRs, including PAR<sub>2</sub>, undergo endocytosis (3, 7). GPCR trafficking is usually studied in cell lines overexpressing receptors. Little is known about agonist-evoked trafficking of endogenous GPCRs in intact tissues or organisms, largely due to the inadequate specificity or sensitivity of GPCR antibodies. To examine agonist-evoked trafficking of PAR<sub>2</sub> in tissues, isolated segments of colon from *Par<sub>2</sub>-mugfp* mice were incubated with trypsin (140 nM), 2F (100 μM), or vehicle (60 min, 37°C). In vehicle-treated colon, PAR<sub>2</sub>-muGFP was principally localized to the basolateral plasma membrane of colonocytes (Fig. 3A and B, arrowheads). Trypsin or 2F stimulated depletion of PAR<sub>2</sub>-muGFP from the plasma membrane and accumulation in intracellular vesicles (Fig. 3A and B, arrows). Vesicles containing PAR<sub>2</sub>-muGFP were costained with an antibody to early endosomal antigen 1 (EEA1) and are thus early endosomes (Fig. 3C and D; *SI Appendix, Fig. S2A*, arrows). Some vesicles were costained with an antibody to Rab7a and are late endosomes (*SI Appendix, Fig. S2B*). Quantification of endocytosis, assessed by the cytosol-plasma membrane pixel intensity, confirmed extensive endocytosis of PAR<sub>2</sub>-muGFP (Fig. 3E and F). Thus, agonists evoke robust endocytosis of endogenous PAR<sub>2</sub> in the intact colon.

**Inflammation-Evoked Trafficking of PAR<sub>2</sub>-muGFP in the Colon.** Little is known about the impact of disease on the subcellular distribution of GPCRs. The continued generation of agonists during chronic disease could induce the redistribution of receptors from the plasma membrane to endosomes. Continued GPCR

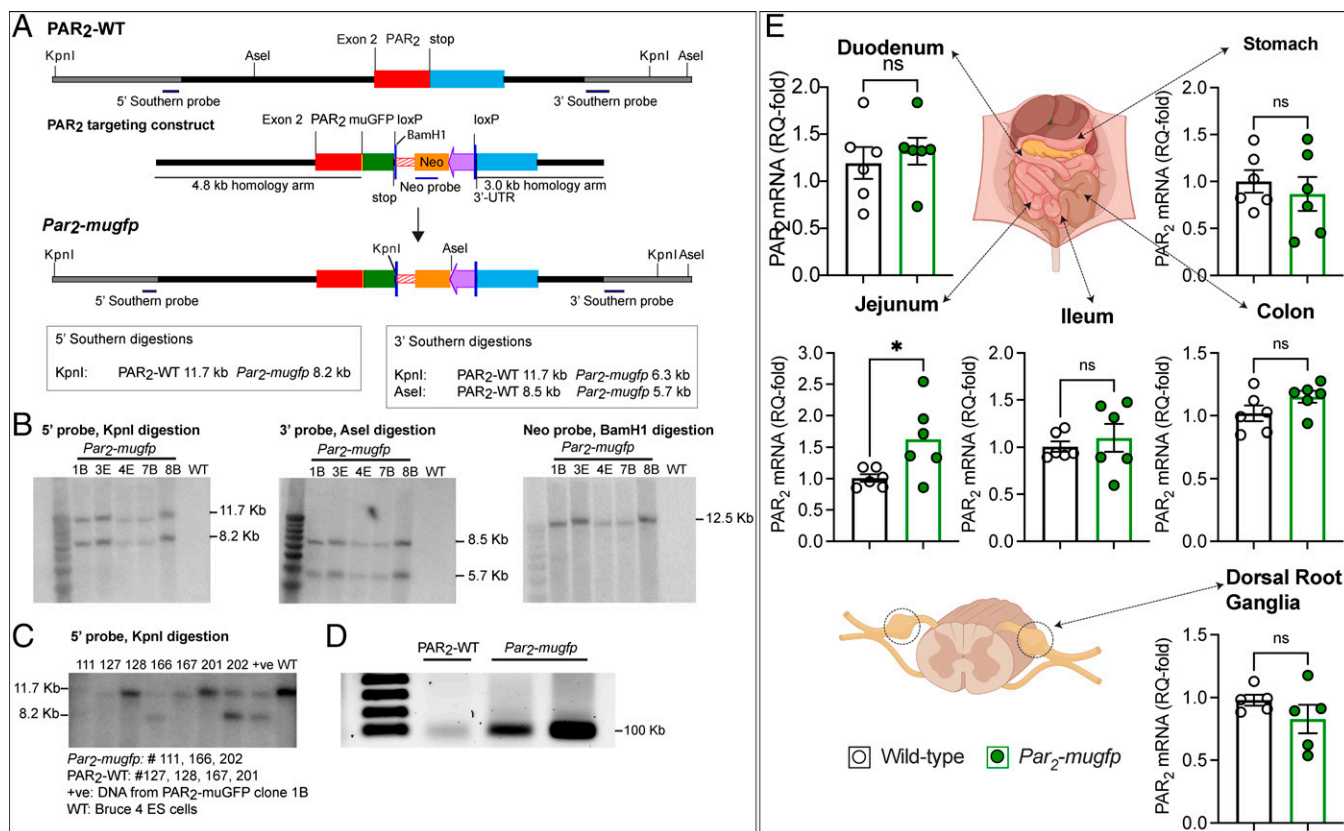


**Fig. 1.** Generation and characterization of *Par2-mugfp* mice. (A) *Par2-mugfp* targeting construct comprising a downstream phosphoglycerine kinase neomycin cassette flanked by *loxP* sites and a downstream *KpnI* site. (B) Southern blot confirming correct targeting. (C) Southern blot and (D) RT-PCR blot confirming *Par2-mugfp* expression in mice. WT, wild-type. (E) Expression of *F2rl1* (*Par2*) mRNA in the digestive tract and DRG of *Par2-mugfp* and wild-type mice determined by qRT-PCR.  $n = 6$  mice. Mean  $\pm$  SEM; ns, nonsignificant. \* $P < 0.05$ , Student's  $t$  test.

signaling from intracellular compartments (e.g., endosomes) underlies disease processes, including persistent pain (5–9). This has implications for therapy, because GPCRs in endosomes might be inaccessible to antagonists that fail to penetrate the plasma and endosomal membranes (e.g., monoclonal antibodies) or cannot effectively engage conformations of GPCRs within multiprotein signaling complexes in acidic endosomes (32). Thus, an understanding of disease-evoked trafficking of GPCRs is required for the design of optimal therapies. We investigated whether  $PAR_2$  redistributes to endosomes of colonocytes during colitis, when multiple host and microbiome proteases are activated (20, 22, 23, 25).

*Par2-mugfp* mice were treated with 3% dextran sulfate sodium (DSS) in drinking water for 7 d to induce mucosal inflammation of the colon. Controls received plain water. DSS induced signs of colitis, including fecal blood, diarrhea, weight loss, and colon shortening (Fig. 4A and B).  $PAR_2$ -muGFP was localized at the basolateral plasma membrane of colonocytes in control mice (Fig. 4C, arrowheads). At 24 h after DSS treatment,  $PAR_2$ -muGFP was depleted from the plasma membrane and prominently detected in intracellular vesicles of colonocytes (Fig. 4C, arrows). *Par2-mugfp* mice were also treated with trinitrobenzene sulphonic acid (TNBS; 4 mg/mL in 0.9% NaCl and 50% ethanol, 150- $\mu$ L enema) to induce transmural inflammation of the colon. Control mice received vehicle (0.9% NaCl and 50% ethanol). After 72 h, TNBS-treated mice had extensive transmural inflammation, with mucosal and submucosal infiltration of neutrophils (Fig. 4D and E).  $PAR_2$ -muGFP was prominently detected in intracellular vesicles (Fig. 4F, arrows) and also present at the plasma membrane (Fig. 4F, arrowheads) of colonocytes. In regions of marked inflammation and mucosal

disruption,  $PAR_2$ -muGFP was detected in immune cells of the mucosa (Fig. 4G, arrowheads) and EEA1-positive early endosomes of colonocytes (Fig. 4G, arrows).

In two preclinical models of IBD,  $PAR_2$ -muGFP redistributes from the plasma membrane to endosomes of colonocytes. This redistribution is likely attributable to the activation of proteases in the inflamed colon.

**Mechanism and Pathway of  $PAR_2$  Trafficking in Colonocytes.** Activated  $PAR_2$  undergoes clathrin-mediated endocytosis and traffics to early endosomes and lysosomes (13).  $PAR_2$  ubiquitination is necessary for lysosomal targeting (33). Recovery of cellular responsiveness requires  $G\beta\gamma$ -dependent activation of protein kinase D, which liberates newly synthesized  $PAR_2$  from the Golgi apparatus and stimulates translocation to the plasma membrane (34, 35).

We used enhanced bystander bioluminescence resonance energy transfer (ebBRET), which capitalizes on the affinity of *Renilla*-tagged proteins, to study the intracellular trafficking of  $PAR_2$  in T84 human colon carcinoma cells (26). To assess  $PAR_2$  endocytosis, we coexpressed  $PAR_2$  coupled to *Renilla* luciferase 8 (Rluc8) and the plasma membrane marker CAAX coupled to *Renilla* GFP (RGFP) or the early endosome marker Rab5a coupled to tandem (td) RGFP. 2F (100  $\mu$ M) decreased BRET (i.e., proximity) between  $PAR_2$ -Rluc8 and RGFP-CAAX and increased BRET between  $PAR_2$ -Rluc8 and tdRGFP-Rab5a, consistent with endocytosis (Fig. 5B and C). Hypertonic (0.45 M) sucrose, dominant-negative dynamin (Dnm) K44A, and Dnm2 siRNA inhibited endocytosis of  $PAR_2$  (Fig. 5D–G). Dnm2 was the predominant Dnm isoform in T84 cells, which expressed Dnm1 and Dnm3 messenger RNA (mRNA) at lower



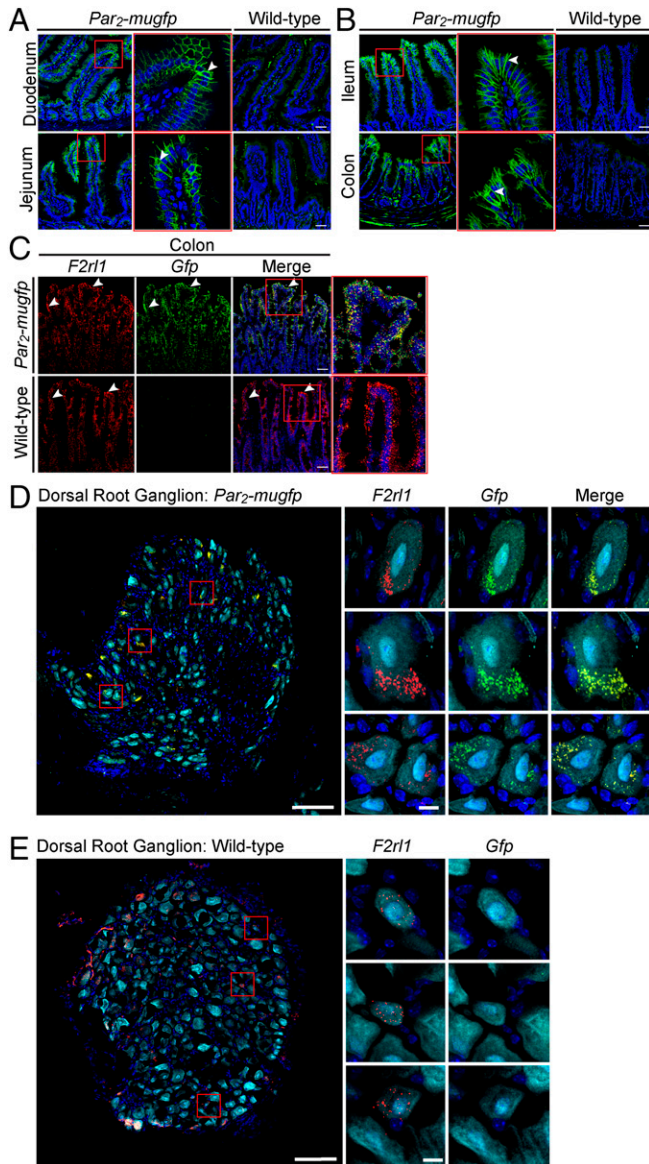


**Fig. 2.** Localization of PAR<sub>2</sub>-muGFP in the intestine and DRG by immunofluorescence and RNAScope in situ hybridization. (A and B) Localization of GFP immunoreactivity in duodenum and jejunum (A) and ileum and colon (B) of *Par<sub>2</sub>-muGFP* and wild-type mice. (C) RNAScope localization of *F2r11* and *Gfp* mRNA in colon of *Par<sub>2</sub>-muGFP* and wild-type mice. Arrowheads indicate immunoreactivity at the basolateral membrane of epithelial cells and mRNA expression within epithelial cells. (D and E) RNAScope localization of *F2r11* and *Gfp* mRNA in DRG of *Par<sub>2</sub>-muGFP* (D) and wild-type (E) mice. (Scale bars, 10  $\mu$ m.) Representative images, independent experiments. *n* = 5 mice.

levels (SI Appendix, Fig. S3A). siRNA knockdown of *Dnm2* was verified by qRT-PCR (SI Appendix, Fig. S3B).

To study the intracellular trafficking of PAR<sub>2</sub>, we expressed BRET1 sensors for PAR<sub>2</sub> and subcellular compartments in HEK293T cells (Fig. 5A), where BRET1 responses were larger. 2F (10  $\mu$ M) and trypsin (100 nM) decreased BRET between PAR<sub>2</sub>-Rluc8 and Venus-KRas (plasma membrane) and increased BRET between PAR<sub>2</sub>-Rluc8 and Venus-Rab5a (early endosome) (Fig. 5 H–K; SI Appendix, Fig. S4 A–D). BRET between PAR<sub>2</sub>-Rluc8 and Venus-Rab7a (late endosome) was unaffected (Fig. 5 L and M; SI Appendix, Fig. S4 E and F). 2F increased BRET between PAR<sub>2</sub>-Rluc8 and Venus-Giantin (*cis*-Golgi) and caused a transient decrease and then a sustained increase in BRET between PAR<sub>2</sub>-Rluc8 and YFP-TGN-38

(*trans*-Golgi) (Fig. 5 N–Q). Trypsin did not affect BRET between PAR<sub>2</sub>-Rluc8 and Venus-Giantin but caused a transient decrease in BRET between PAR<sub>2</sub>-Rluc8 and YFP-TGN-38 (SI Appendix, Fig. S4 G–J). 2F and trypsin stimulated BRET between PAR<sub>2</sub>-Rluc8 and Venus-Rab11a (recycling endosomes) (Fig. 5 R and S; SI Appendix, Fig. S4 K and L). *DnmK44A* inhibited the recruitment of PAR<sub>2</sub> to most compartments.

To determine whether fusion to muGFP affects PAR<sub>2</sub> trafficking, we expressed PAR<sub>2</sub>-muGFP in HEK293T cells expressing markers of early and late endosomes and the Golgi apparatus tagged with red fluorescent protein (RFP) and localized PAR<sub>2</sub> and markers by confocal microscopy. 2F (10  $\mu$ M, 30 min) stimulated trafficking of PAR<sub>2</sub>-muGFP from the plasma membrane to early endosomes (Fig. 5T; SI Appendix, Fig. S5). PAR<sub>2</sub>-muGFP was not detected in late endosomes or the Golgi apparatus by microscopy (Fig. 5U; SI Appendix, Fig. S6).

**Assembly of a PAR<sub>2</sub> Signaling Complex with G $\alpha$  or  $\beta$ ARR.** GPCRs can assemble G $\alpha$  and  $\beta$ ARR signaling complexes in endosomes, which enable sustained signaling of internalized receptors (3, 4, 36, 37). Within endosomes, G $\alpha$  subunits can transduce signals and  $\beta$ ARRs serve as scaffolds that organize GPCRs and signaling enzymes. Because agonists stimulated trafficking of PAR<sub>2</sub> to early endosomes of T84 and HEK293T cells, we examined the assembly of signaling complexes in this compartment. The activation of G $\alpha_q$ , G $\alpha_i$ , and G $\alpha_s$  was studied using ebBRET to detect recruitment of mini-G $\alpha$  (mG $\alpha$ ) coupled to Rluc8 to RGFP-CAAX or tdRGFP-Rab5a (Fig. 6A). mG $\alpha$  proteins are N-terminally truncated G $\alpha$  proteins that freely diffuse within the cytosol and bind to active conformations of GPCRs, which reflects G $\alpha$  activation. mG $\alpha_{sq}$  and mG $\alpha_{si}$  were developed by mutating mG $\alpha_s$  residues to equivalent G $\alpha_q$  and G $\alpha_i$  residues. Recruitment of  $\beta$ ARR was assessed by measuring ebBRET between Rluc2- $\beta$ ARR2 and RGFP-CAAX or tdRGFP-Rab5a (Fig. 6A). In T84 cells, 2F (100  $\mu$ M) stimulated the rapid recruitment of mG $\alpha_{sq}$ , mG $\alpha_{si}$ , or  $\beta$ ARR2 to the plasma membrane and endosomes, although  $\beta$ ARR2 recruitment to endosomes was slower and more sustained than recruitment to the plasma membrane (Fig. 6 B–D). mG $\alpha_s$  was not recruited to the plasma membrane or endosomes.

We studied the mechanisms of assembly of signaling complexes in HEK293T cells. 2F (100  $\mu$ M) and trypsin (100 nM) stimulated the recruitment of mG $\alpha_{sq}$ , mG $\alpha_{si}$ , and  $\beta$ ARR2 to the plasma membrane and endosomes of HEK293T cells (SI Appendix, Fig. S7 A–F). Whereas the recruitment of mG $\alpha_{sq}$ , mG $\alpha_{si}$  and  $\beta$ ARR2 at the plasma membrane declined over 1,400 s, their recruitment to endosomes increased or was sustained. Hypertonic sucrose delayed the recruitment of mG $\alpha_{sq}$ , mG $\alpha_{si}$ , and  $\beta$ ARR2 to the plasma membrane, although ebBRET signals ultimately reached those of controls. In contrast, hypertonic sucrose abolished recruitment of mG $\alpha_{sq}$ , mG $\alpha_{si}$ , and  $\beta$ ARR2 to endosomes.

Conventional BRET is limited to measuring the proximity between two proteins. To simultaneously measure the proximity between PAR<sub>2</sub>, an effector (mG $\alpha$  or  $\beta$ ARR), and a localization marker, we used NanoLuc Binary Technology (38), NanoBiT BRET (nbBRET) (Fig. 6E). A split luciferase assay was developed in which PAR<sub>2</sub> was tagged at the C terminus with the natural peptide fragment of NanoLuc (NP, a 13-residue NanoLuc fragment), and a plasma membrane or endosomal marker was tagged with the large BiT fragment of NanoLuc (LgBiT-CAAX or LgBiT-FYVE, respectively). Luminescence occurs from a complex between PAR<sub>2</sub>-NP and LgBiT-CAAX or LgBiT-FYVE, which serves as an energy donor for fluorophore-tagged mG $\alpha$  or  $\beta$ ARR. In T84 colonocytes, 2F (100  $\mu$ M) increased nbBRET between PAR<sub>2</sub>, mG $\alpha_{si}$ , mG $\alpha_{sq}$ , or  $\beta$ ARR1 and markers of the plasma membrane or endosome (Fig. 6 F–H). In HEK293T cells, 2F and trypsin also stimulated nbBRET

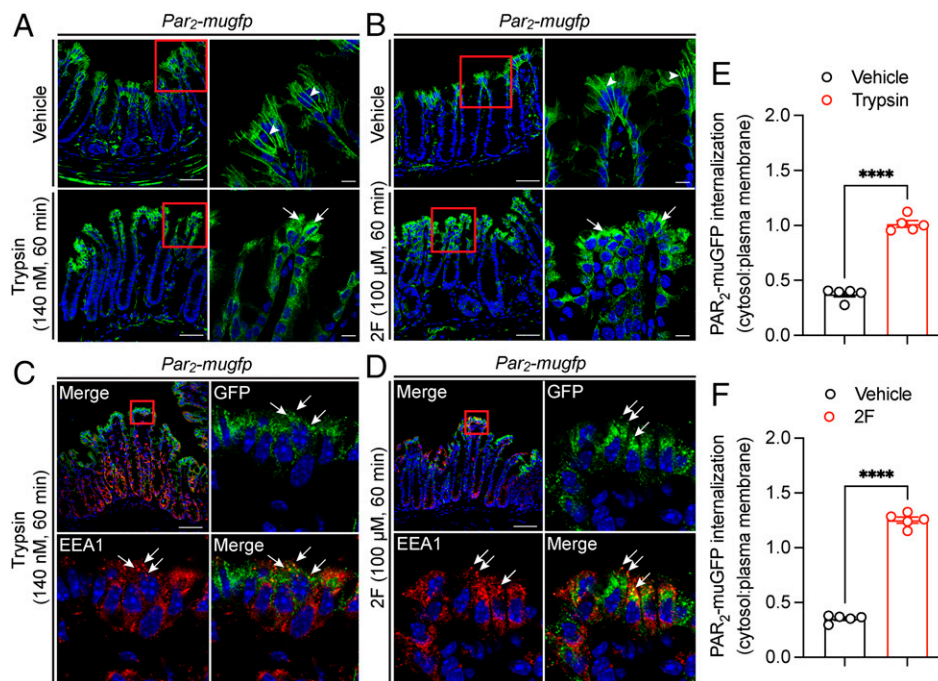


**Fig. 3.** Agonist-evoked endocytosis of PAR<sub>2</sub>-muGFP in the colon. (A and B) Localization of GFP immunoreactivity in isolated segments of colon from *Par<sub>2</sub>-mugfp* mice incubated with vehicle, trypsin (A, 140 nM, 60 min) or 2F (B, 100 μM, 60 min). (C and D) Colocalization of GFP and EEA1 in segments treated with trypsin (C) or 2F (D). Arrowheads denote plasma membrane, and arrows denote endosomes. (Scale bar, 10 μm.) Representative images and independent experiments are shown ( $n = 5$  mice). (E and F) Quantification of PAR<sub>2</sub>-muGFP internalization after vehicle, trypsin (E), or 2F (F) (cytosol–plasma membrane pixel intensity). Mean  $\pm$  SEM;  $n = 5$  mice. \*\*\*\* $P < 0.0001$ , Student's  $t$  test.

between PAR<sub>2</sub>, mGα<sub>si</sub>, mGα<sub>sq</sub>, or βARR1 and CAAX or FYVE (Fig. 6 I–K; *SI Appendix, Fig. S8 A–H*). Recruitment of mGα and βARR to early endosomes lagged behind recruitment to the plasma membrane. nbBRET signals were maintained for at least 1,200 s, suggesting assembly of stable PAR<sub>2</sub>/mGα or PAR<sub>2</sub>/βARR complexes. Hypertonic sucrose inhibited agonist-stimulated assembly of PAR<sub>2</sub>, mGα<sub>si</sub>, mGα<sub>sq</sub>, or βARR1 complexes in early endosomes (*SI Appendix, Fig. S8 A, B, F, and G*). DynK44A had similar inhibitory effects on signalosome assembly but to a lesser extent (*SI Appendix, Fig. S8 C, D, G, and H*). The PAR<sub>2</sub> antagonist GB88 prevented 2F and trypsin-stimulated signalosome assembly in endosomes of HEK293T cells (*SI Appendix, Fig. S8 I and J*). Immunofluorescence and confocal microscopy confirmed localization of HA-LgBiT-CAAX at the plasma membrane and HA-LgBiT-FYVE in endosomes (*SI Appendix, Fig. S8K*).

In unstimulated HEK293T cells, immunoreactive PAR<sub>2</sub> was localized to the plasma membrane, and immunoreactive Gα<sub>q</sub> and YFP-βARR1/2 were cytosolic (Fig. 6L). In cells exposed to 2F (10 μM, 30 min), PAR<sub>2</sub>, Gα<sub>q</sub>, and YFP-βARR1/2 were colocalized in early endosomes.

Our results suggest that agonists induce assembly of a signal complex comprising PAR<sub>2</sub> and Gα<sub>q</sub>, Gα<sub>i</sub>, or βARR1/2 in early endosomes. This process requires Dnm-dependent endocytosis of PAR<sub>2</sub>.

**PAR<sub>2</sub> Endocytosis and the Colonic Epithelial Barrier.** Tight junctions between colonocytes form a barrier that prevents the ingress of proinflammatory macromolecules and microbes from the lumen. Alterations in tight junction structure contribute to impaired barrier function and inflammation in IBD. PAR<sub>2</sub> agonists promote paracellular permeability of the colon (39) by a mechanism that involves βARR-dependent activation of ERK1/2 and redistribution of ZO1 and occludin from tight junctions (3, 26), suggesting a role for endosomal PAR<sub>2</sub> signaling.

Analysis of the expression of Dnm isoforms in the mouse colon by RNAScope in situ hybridization and RT-qPCR revealed prominent expression of *Dnm2* in colonocytes, whereas *Dnm1* and *Dnm3* mRNA were largely confined to the enteric nervous system (Fig. 7 A and B). When applied to the basolateral surface of T84 monolayers, trypsin (100 nM) and 2F (10 μM) decreased transepithelial electrical resistance (TEER) after 6 h, consistent with redistribution of tight junctional proteins and increased paracellular permeability (Fig. 7C). The PAR<sub>2</sub> antagonist GB88 prevented these effects, confirming a role for PAR<sub>2</sub>. *Dnm2* siRNA similarly prevented the effects of trypsin and 2F on TEER, implicating a requirement for PAR<sub>2</sub> endocytosis (Fig. 7 D and E).

**PAR<sub>2</sub> Endocytosis, Colonic Inflammation, and Pain.** To ascertain whether *Dnm2* could contribute to colonic inflammation in vivo, we administered *Dnm2* or control small hairpin RNA (shRNA) into the colon of *Par<sub>2</sub>-mugfp* mice. After 48 h, RNAScope in situ hybridization revealed ~50% knockdown of *Dnm2* mRNA in colonocytes of mice treated with *Dnm2* shRNA compared to control shRNA (Fig. 8 A and B). To assess the effects of *Dnm2* knockdown on PAR<sub>2</sub>-mediated colonic inflammation and pain, we administered 2F (100 μM) or vehicle into the colon by enema (150 μL). Endocytosis of PAR<sub>2</sub>-muGFP, colonic levels of proinflammatory factors, and colonic nociception were assessed. In mice receiving control shRNA, 2F stimulated endocytosis of PAR<sub>2</sub>-muGFP in colonocytes after 6 h; *Dnm2* shRNA inhibited endocytosis (Fig. 8C). In control mice, 2F increased mRNA levels of tumor necrosis factor α (TNF-α), C-X-C motif chemokine ligand 1 (CXCL1), and interleukin-1β (IL-1β) in the colon (Fig. 8 D–F). Intracolonic 2F decreased withdrawal responses of the abdomen to calibrated von Frey filaments from 1 to 5 h, which indicates hyperalgesia (Fig. 8 G and H). These results are consistent with the known proinflammatory and pronociceptive actions of PAR<sub>2</sub> in the colon (7, 22, 30). *Dnm2* shRNA inhibited



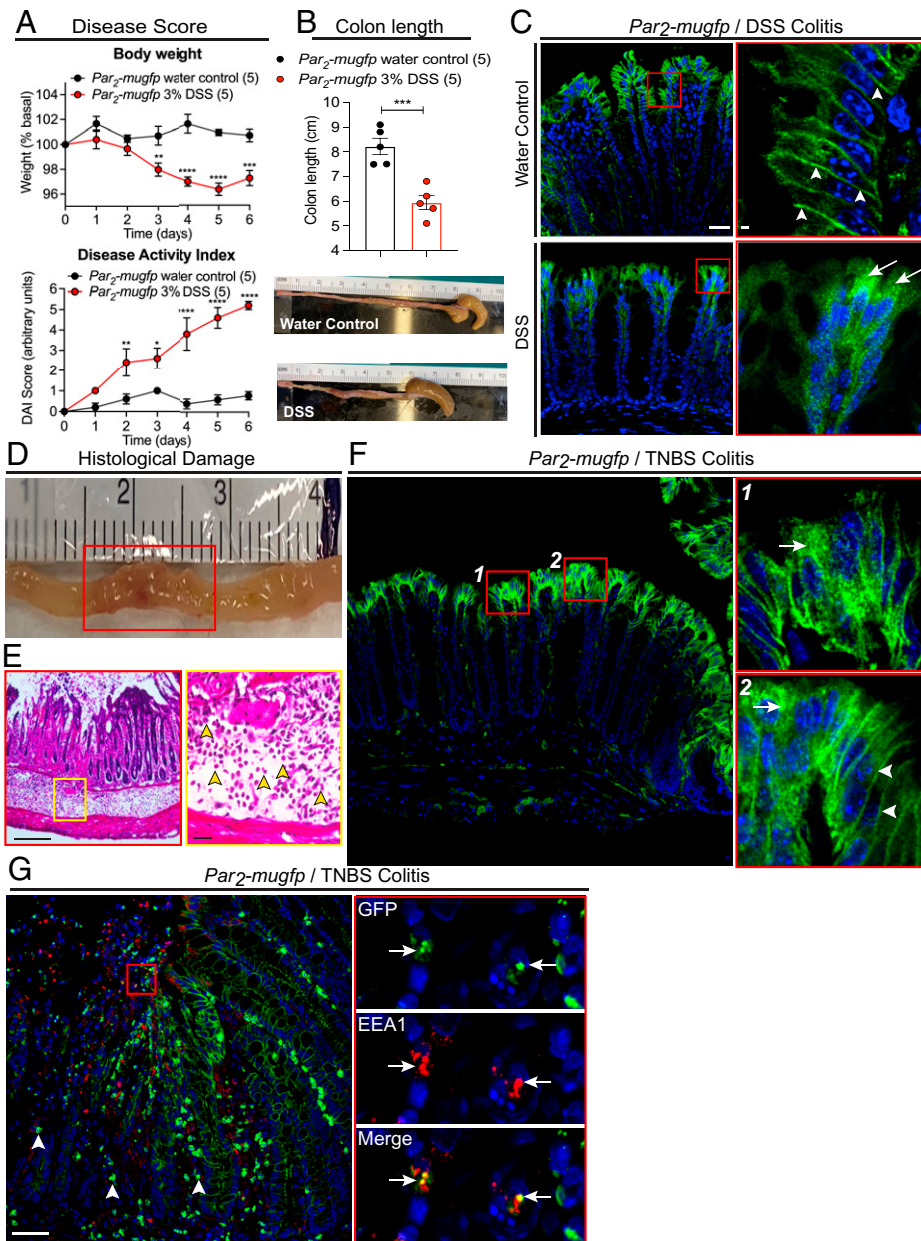


**Fig. 4.** Colitis-evoked endocytosis of PAR<sub>2</sub>-muGFP. (A–C) DSS colitis in *Par<sub>2</sub>-mugfp* mice. (A) Body weight and disease activity index (DAI) after DSS or water (control). (B) Colon length after DSS or water. Mean ± SEM, *n* = 5 mice. \**P* < 0.05, \*\**P* < 0.01, \*\*\**P* < 0.001, and \*\*\*\**P* < 0.0001 compared to water, two-way ANOVA, Tukey's test (A), and Student's *t* test (B). (C) Redistribution of PAR<sub>2</sub>-muGFP from the plasma membrane (arrowheads) to endosomes (arrows) after DSS. (D–F) TNBS colitis in *Par<sub>2</sub>-mugfp* mice. (D) Grossly inflamed colon. (E) Histological sections showing infiltration of neutrophils in the submucosa (yellow arrowheads). (F) Redistribution of PAR<sub>2</sub>-muGFP from the plasma membrane to endosomes after TNBS. (G) Localization of PAR<sub>2</sub>-muGFP in infiltrating immune cells (arrowheads) and colocalization of GFP and EEA1 in colonocytes (arrows). (Scale bars, 10 μm.) Representative images and independent experiments are shown (*n* = 5 mice).

2F-stimulated inflammation and nociception. The pronociceptive response to intracolonic 2F was similar in *Par<sub>2</sub>-mugfp* and wild-type mice but was attenuated in *Par<sub>2</sub>Na<sub>v</sub>1.8* mice that lack PAR<sub>2</sub> in Na<sub>v</sub>1.8-positive nociceptors (7) (Fig. 8 *I* and *J*). These results implicate PAR<sub>2</sub> on Na<sub>v</sub>1.8-positive neurons in colonic pain and are in line with our report that proteases induce somatic nociception by activating PAR<sub>2</sub> on Na<sub>v</sub>1.8 neurons (7). The intraplantar injection of trypsin (140 nM, 10 μL) induced mechanical allodynia to a similar degree in the ipsilateral paw but not contralateral paw of *Par<sub>2</sub>-mugfp* and wild-type mice (SI Appendix, Fig. S9 *A* and *B*). Mechanical allodynia was significantly attenuated in *Par<sub>2</sub><sup>-/-</sup>* mice, confirming a role for PAR<sub>2</sub>.

IL-8 is proinflammatory cytokine that is released by colonocytes (40). To examine whether PAR<sub>2</sub> evokes inflammation of the human colon, we incubated explants of normal human colonic mucosa with 2F (10 μM, 4 h) and measured IL-8 release into culture medium. 2F stimulated IL-8 release (Fig. 8*K*). Preincubation of explants with dyngo4a (30 μM), a Dnm inhibitor, blocked PAR<sub>2</sub>-mediated IL-8 release.

These results suggest that PAR<sub>2</sub> agonists increase paracellular permeability, stimulate cytokine and chemokine release from colonocytes, and sensitize colonic nociceptors. These proinflammatory and pronociceptive actions require Dnm-mediated endocytosis of PAR<sub>2</sub>.

## Discussion

Although proteases and PAR<sub>2</sub> are implicated in inflammatory diseases, the impact of inflammation on the subcellular distribution and function of PAR<sub>2</sub> has not been investigated. The use of knockin mice expressing PAR<sub>2</sub> fused to muGFP allowed examination of the effects of inflammation on the subcellular trafficking of PAR<sub>2</sub> with high resolution. We detected a major redistribution of PAR<sub>2</sub> from the basolateral membrane to early endosomes of colonocytes in two preclinical models of IBD, which is likely due to increased proteolytic activity in the inflamed colon. By using BRET to probe the formation and composition of PAR<sub>2</sub> signaling complexes, we found that agonists induce the assembly of signalosome comprising PAR<sub>2</sub> and Gα<sub>i</sub>, Gα<sub>q</sub> or βARR1/2 in colonic epithelial cells. Our results suggest that Dnm2-mediated endocytosis of PAR<sub>2</sub> in the colon is necessary for paracellular permeability, generation of proinflammatory cytokines and chemokines, and sensitization of colonic nociceptors (Fig. 7E).

**PAR<sub>2</sub> Localization and Trafficking.** Mice expressing fluorescent opioid receptors have been extensively used to analyze tissue distribution and the effects of endogenous agonists and drugs on receptor trafficking (41, 42). The use of knockin mice in which *Par<sub>2</sub>* was replaced by *Par<sub>2</sub>-mugfp* enabled specific and high-resolution analysis of the tissue distribution and subcellular trafficking of PAR<sub>2</sub> in inflamed tissues. Fusion of muGFP did not affect PAR<sub>2</sub> signaling and trafficking in cell lines, and mRNA encoding *Par<sub>2</sub>-mugfp* was expressed at similar levels to endogenous *Par<sub>2</sub>* in most regions of the digestive tract and sensory ganglia. PAR<sub>2</sub> agonists induced comparable somatic and visceral nociception in *Par<sub>2</sub>-mugfp* and wild-type mice. These findings suggest that PAR<sub>2</sub>-muGFP functions normally. Within the digestive tract, PAR<sub>2</sub>-muGFP immunoreactivity was prominently localized to the basolateral plasma membrane of epithelial cells lining the small and large intestine. RNAScope using probes to *F2rl1* and *Gfp* confirmed expression by enterocytes and colonocytes. The lack of GFP immunoreactivity and mRNA in wild-type mice verified selectivity. The detection of PAR<sub>2</sub> in intestinal epithelial cells confirms reports using receptor antibodies and functional assays (27, 43).

Detection of PAR<sub>2</sub> in DRG neurons required the sensitivity of RNAScope in situ hybridization, which revealed expression in a subset of neurons, in agreement with other reports (7, 44). The activation of PAR<sub>2</sub> in DRG nociceptors stimulates the release of substance P and calcitonin gene-related peptide, which mediate neurogenic inflammation in peripheral tissues and the central transmission of pain (28, 29). Proteases may cause pain in the colon directly by activating PAR<sub>2</sub> on nociceptors or indirectly by activating PAR<sub>2</sub> on colonocytes and stimulating release of pronociceptive factors. The observation that deletion of PAR<sub>2</sub> from Na<sub>v</sub>1.8 neurons blunts colonic nociception supports a primary role for neuronal PAR<sub>2</sub>. Deletion of *Par<sub>2</sub>* from Na<sub>v</sub>1.8 neurons also attenuates protease-evoked somatic nociception (7, 44).

The identity of the proteases that activate PAR<sub>2</sub> and stimulate endocytosis was not addressed in the current study. Protease probes and proteomics have been used to identify serine and cysteine proteases that are activated in the colon of mice with colitis and patients with IBD (20–25). These include proteases from immune cells [e.g., neutrophil elastase and cathepsin S (20–22)], proteases from colonocytes [e.g., trypsins (45)], and proteases from the microbiome. An understanding of whether PAR<sub>2</sub> is principally expressed at the apical or basolateral membrane of intestinal epithelial cells has implications for mechanisms of activation. Luminal proteases from epithelial cells, exocrine glands, or colonic bacteria could activate apical PAR<sub>2</sub>, whereas proteases from mucosal immune or epithelial cells could activate PAR<sub>2</sub> at the basolateral membrane. Our

finding of predominant basolateral expression is consistent with reports that basolateral, but not apical, application of PAR<sub>2</sub> agonists increases paracellular permeability (43), although PAR<sub>2</sub> has also been detected at the apical membrane (27).

**PAR<sub>2</sub> Signaling Complexes.** We studied the intracellular trafficking of PAR<sub>2</sub> in colon-derived epithelial cells (T84) and model cell lines (HEK293T) by using BRET to assess the proximity of PAR<sub>2</sub> to subcellular markers and confocal microscopy to localize PAR<sub>2</sub>. Our results show that trypsin and 2F deplete PAR<sub>2</sub> from the plasma membrane and induce accumulation in early endosomes, which were identified using several markers (Rab5a, EEA1, FYVE, and CellLights RFP). Dominant-negative DnmK44A, knockdown of Dnm2 (the principal isoform of T84 cells and colonocytes), and hypertonic sucrose blunted endocytosis of PAR<sub>2</sub>, suggesting a major role for Dnm2. We did not detect PAR<sub>2</sub> in Rab7a-positive late endosomes, possibly due to receptor degradation. 2F, but not trypsin, increased the BRET signal for PAR<sub>2</sub> in the *cis*-Golgi and stimulated a transient decrease and then a sustained increase in the BRET signal in the *trans*-Golgi. The differential effects of 2F and trypsin likely relate to their different mechanisms of PAR<sub>2</sub> activation. Agonist-evoked depletion of PAR<sub>2</sub> from the *trans*-Golgi is consistent with our studies showing that proteases induce Gβγ- and protein kinase D-dependent mobilization of PAR<sub>2</sub> from the Golgi apparatus to the plasma membrane (34, 35). Agonist-evoked translocation of PAR<sub>2</sub> from the plasma membrane to the Golgi apparatus was not prominent, because we detected PAR<sub>2</sub>-muGFP in early endosomes, but not the Golgi apparatus.

Several observations support the hypothesis that PAR<sub>2</sub> agonists induce assembly of a PAR<sub>2</sub> signaling complex with Gα or βARR in early endosomes of T84 and HEK293T cells. eBRET revealed that 2F and trypsin stimulated the recruitment of Gα<sub>q</sub>, Gα<sub>i</sub>, and βARR2 to early endosomes. NbBRET, a split luciferase BRET assay that allows simultaneous measurements of proximity between PAR<sub>2</sub>, an effector (Gα, βARR), and an early endosomal marker, confirmed agonist-evoked recruitment of receptor and effector to early endosomes. Dominant-negative DnmK44A, Dnm2 siRNA, and hypertonic sucrose inhibited the recruitment of PAR<sub>2</sub>, Gα<sub>q</sub>, Gα<sub>i</sub>, and βARR1/2 to endosomes. We also detected PAR<sub>2</sub>, full-length Gα<sub>q</sub>, and βARR in endosomes by microscopy. Further experiments are needed to determine whether a PAR<sub>2</sub>, Gα, and βARR megaplex forms in endosomes. It remains to be determined whether the complex traffics from the plasma membrane to endosomes or PAR<sub>2</sub> recruits Gα and βARR to endosomes. Because GPCRs can form megaplexes with Gα and βARR, the former possibility is more likely. A limitation of our work is that we did not investigate the signals that emanate from internalized PAR<sub>2</sub>. We have previously reported that PAR<sub>2</sub> in endosomes regulates kinases (MEKK1 and ERK1/2) in certain subcellular compartments (3, 7). The endosomal complex was stable during the period of measurement (1,200 s), which might give rise to sustained signals in subcellular compartments that control critical functions of colonocytes, including tight junction assembly and release or proinflammatory and pronociceptive factors. Our results do not exclude the possibility that PAR<sub>2</sub> signals from other organelles, such as the Golgi apparatus, as is the case for thyroid-stimulating hormone receptors and opioid receptors (10, 11). Proteases of late endosomes, including cathepsin S and legumain, can activate PAR<sub>2</sub> even in acidic conditions, which could facilitate receptor activation in other subcellular compartments (17, 22). However, the most parsimonious explanation of our results is that signalosomes comprising PAR<sub>2</sub> and Gα<sub>q</sub>, Gα<sub>i</sub>, or βARR1/2 assemble predominantly in early endosomes.

**Endosomal PAR<sub>2</sub> Signaling, Colonic Inflammation, and Pain.** Our results suggest that endosomal signaling of PAR<sub>2</sub> in the colon increases paracellular permeability and evokes secretion of cytokines and chemokines, which would be expected to amplify



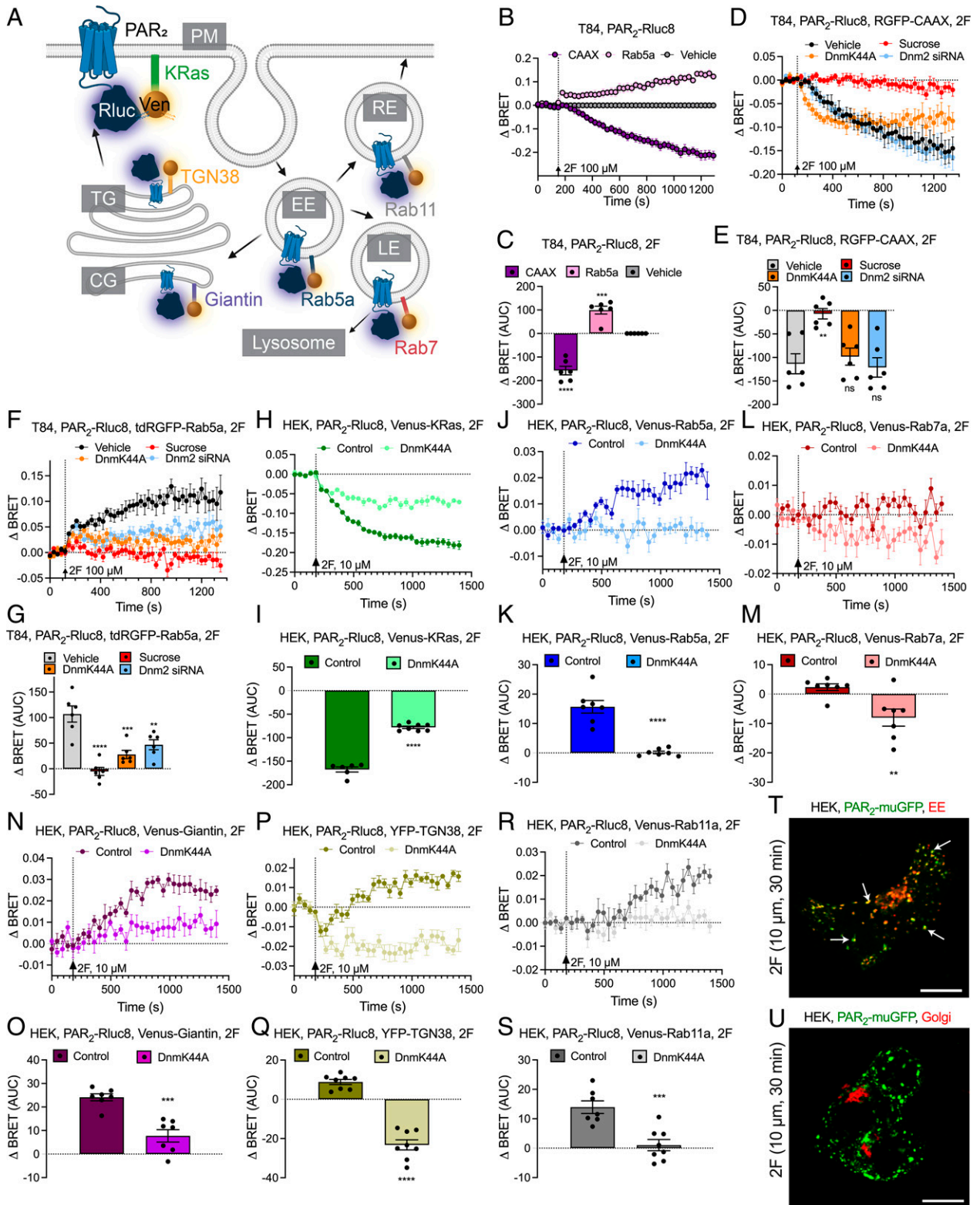


**Fig. 5.** PAR<sub>2</sub> trafficking to endosomes. (A) BRET assays of the proximity between PAR<sub>2</sub>-Rluc8 and Venus- or YFP-tagged proteins resident to plasma membrane (PM; CAAX or KRas), early endosomes (EE; Rab5a), late endosomes (LE; Rab7a), recycling endosomes (RE; Rab11a), *cis*-Golgi (CG; giantin), or *trans*-Golgi (TG; TGN38). (B–G) Effects of 2F (100 μM) on translocation of PAR<sub>2</sub>-Rluc8 from the plasma membrane (RGFP-CAAX) to early endosomes (tdRGFP-Rab5a) of T84 cells treated with vehicle, hypertonic sucrose, or DnmK44A or Dnm2 siRNA. (H–S) Effects of 2F (10 μM) on translocation of PAR<sub>2</sub>-Rluc8 from the plasma membrane [KRas-Venus (H and I)] to early endosomes [Rab5a-Venus (J and K)], late endosomes [Rab7a-Venus (L and M)], *cis*-Golgi [giantin-Venus (N and O)], *trans*-Golgi [TGN38-YFP (P and Q)], and recycling endosomes [Rab11-Venus (R and S)] in HEK293T cells. Cells were transfected with DnmK44A or untransfected (control). AUC, area under the curve. Mean ± SEM; n = 6–11 independent experiments. \*\*P < 0.01, \*\*\*P < 0.001, and \*\*\*\*P < 0.0001, one-way ANOVA or Tukey's test. (T and U) Localization of PAR<sub>2</sub>-muGFP and CellLight markers of early endosomes (T) and the Golgi complex (U) in HEK293T cells. Arrows denote colocalization of PAR<sub>2</sub>-muGFP and marker of early endosomes. Representative images are shown. (Scale bars, 10 μm.)

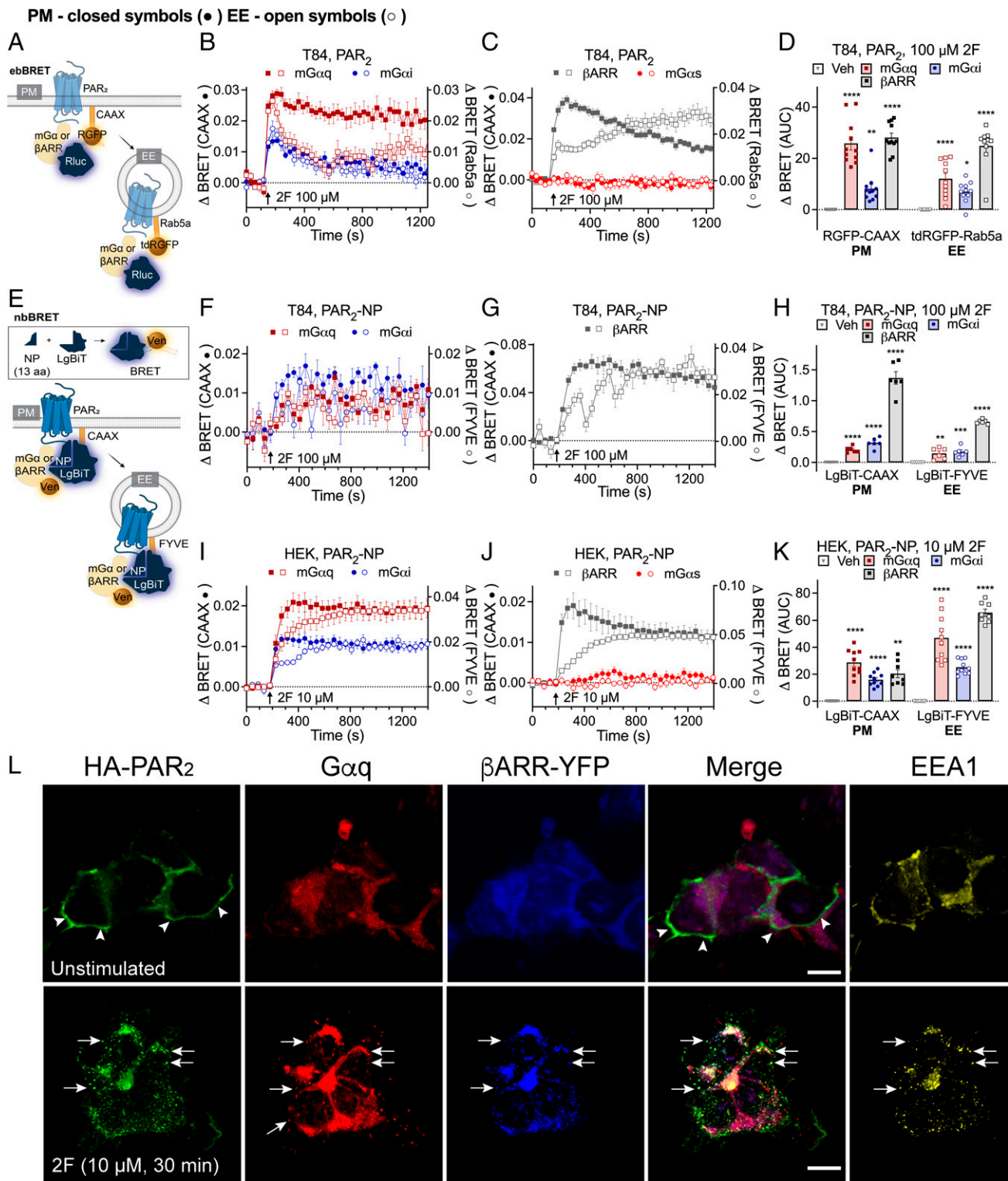


**Fig. 6.** PAR<sub>2</sub>, Gα and βARR signalosome assembly in endosomes. (A) EbBRET assays of proximity between effector (Gα; βARR) and proteins resident to plasma membrane (PM; CAAX) or early endosomes (EE; Rab5a). (B–D) Effects of 2F (100 μM) on the recruitment of mGα<sub>sq</sub>, mGα<sub>si</sub>, βARR2 or mGα<sub>si</sub> negative control (C) to the plasma membrane (RGFP-CAAX, left axis, closed symbols) or early endosomes (tdRGFP-Rab5a, right axis, open symbols) of T84 cells, and (D) area under the curve (AUC). (E) NbBRET uses luciferase split into two fragments to detect BRET between receptor and effector (PAR<sub>2</sub> and mGα or βARR) for proteins resident to the PM (CAAX) or early endosomes (FYVE). (F–H) Effects of 2F (100 μM) on recruitment of mGα<sub>sq</sub>, mGα<sub>si</sub> (F) or βARR1 (G) to the plasma membrane (LgBiT-CAAX) or early endosomes (LgBiT-FYVE) of T84 cells, and (H) AUC. (I–K) Effects of 2F (10 μM) on recruitment of mGα<sub>sq</sub>, mGα<sub>si</sub> (I), βARR1 or mGα<sub>si</sub> (J) to the PM (LgBiT-CAAX) or early endosomes (LgBiT-FYVE) of HEK293T cells. (K) AUC. Mean ± SEM. *n* = 6–11 independent experiments. \**P* < 0.05, \*\**P* < 0.01, \*\*\**P* < 0.001, and \*\*\*\**P* < 0.0001. (D and K) One-way ANOVA with Dunnett's (D) or Holm–Šidák's (K) test compared to vehicle. (H) Unpaired *t* test. (L) Localization of immunoreactive HA-PAR<sub>2</sub>, Gα<sub>q</sub> and EEA1 plus YFP-βARR1 and YFP-βARR2 in HEK293T cells. Cells were unstimulated or incubated with 2F (10 μM, 30 min). Arrowheads, plasma membrane. Arrows, colocalization of HA-PAR<sub>2</sub>, Gα<sub>q</sub> and YFP-βARR1 + 2 in EEA1-positive early endosomes. (Scale bars, 10 μm.) Representative images from *n* = 5 experiments are shown.



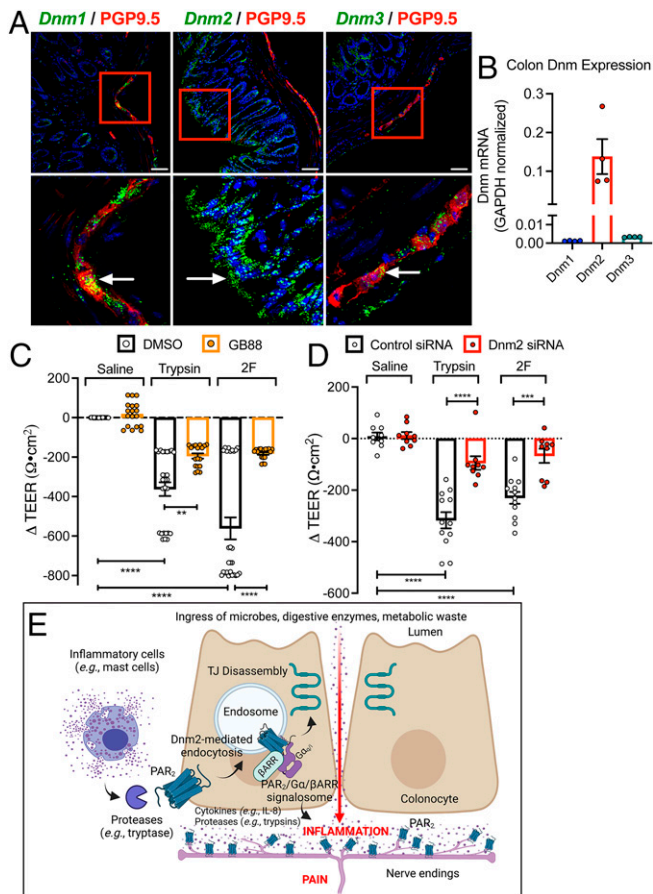


**Fig. 7.** PAR<sub>2</sub> endosomal signaling and colonic inflammation and pain. (A) Localization of *Dnm1-3* in mouse colon by RNAScope in situ hybridization. (Scale bars, 50 μm.) Representative images, independent experiments,  $n = 3$  mice. (B) Expression of *Dnm1-3* in mouse colon by qRT-PCR.  $n = 4$  mice. (C) Effects of trypsin (100 nM), 2F (10 μM), or vehicle (saline, control) on TEER of T84 cells after 6 h. Cells were preincubated with GB88 (PAR<sub>2</sub> antagonist) or vehicle (DMSO, control). (D) Effects of trypsin (100 nM), 2F (10 μM), or vehicle (saline, control) on TEER of T84 cells after 5 h. Cells were preincubated with Dnm2 or control siRNA. Mean ± SEM.  $^{**}P < 0.01$ ,  $^{***}P < 0.001$ , and  $^{****}P < 0.0001$  by one-way ANOVA, Tukey's test, or Student's  $t$  test. (E) Proposed mechanism by which proteases (e.g., trypsin) from mucosal inflammatory cells (e.g., mast cells) activate PAR<sub>2</sub> at the basolateral membrane of colonocytes to evoke PAR<sub>2</sub> endocytosis and assembly of a PAR<sub>2</sub>, Gα, and βARR signalosome in endosomes. Endosomal signaling causes disassembly of tight junctions (TJ) and release of proinflammatory cytokines (e.g., IL-8) and possibly proteases (e.g., trypsin) from colonocytes. The ingress of microbes, proteases, and metabolites from the colonic lumen, and the release of cytokines and proteases from colonocytes, cause inflammation and pain. Proteases activate PAR<sub>2</sub> on nociceptive terminals in the colon to cause pain.

inflammation. In two preclinical mouse models of IBD, PAR<sub>2</sub> was depleted from the basolateral plasma membrane of colonocytes and prominently detected in cytosolic vesicles, including early endosomes. The proteolytic environment of the inflamed intestine is likely to activate PAR<sub>2</sub> and trigger endocytosis and sustained endosomal signaling. In health, tight junctions between colonocytes maintain a barrier that prevents the ingress of macromolecules and microbes from the colonic lumen into the mucosa, which protects against inflammation. Disruption of the barrier would be expected to promote inflammation. When applied to the basolateral surface, trypsin and 2F decreased electrical resistance of polarized monolayers of T84 cells, consistent with a loss of barrier function. The finding that a PAR<sub>2</sub> antagonist and Dnm2 siRNA inhibited this effect suggests a major role for PAR<sub>2</sub> endocytosis and endosomal signaling in redistribution of tight junctional

proteins and loss of barrier function. We previously reported that PAR<sub>2</sub> agonists, including mast cell tryptase, stimulate a redistribution of ZO1 and occludin from tight junctions of T84 cells by a mechanism that involves βARRs, MEKK1, and ERK1/2 (26), in line with a role for endosomal signaling of PAR<sub>2</sub> in this process. The observations that Dnm2 knockdown inhibited agonist-induced endocytosis of PAR<sub>2</sub>-muGFP in colonocytes and prevented release or proinflammatory cytokines and chemokines in vivo, and that a Dnm inhibitor blocked PAR<sub>2</sub>-stimulated secretion of IL-8 from biopsy specimens of human colon, further support a role for PAR<sub>2</sub> endocytosis in colitis. Dnm2 knockdown also abrogated 2F-evoked colonic hyperalgesia, a finding that could be secondary to reduced release from colonocytes of cytokines or proteases that sensitize nociceptors. Because deletion of PAR<sub>2</sub> from Na<sub>v</sub>1.8-positive neurons blunted 2F-evoked colonic hyperalgesia, the latter is likely. The identity of colonocyte-derived proteases remains to be determined, although colonocytes express isoforms of trypsin that activate PAR<sub>2</sub> (45). Further studies are required to ascertain whether endocytosis is necessary for other actions of PAR<sub>2</sub> in the intestine, such as inflammation associated with bacterial proteolysis and food allergies (46).

Our findings support the hypothesis that proteases in the inflamed colon evoke the assembly of a PAR<sub>2</sub> complex with Gα or βARR in endosomes (Fig. 7E). Signals that emanate from this complex disrupt tight junctions and promote release of proinflammatory factors that drive inflammation and pain. The influx of proteases from the colonic lumen could further amplify PAR<sub>2</sub>-mediated inflammation and pain. Therapeutic targeting of PAR<sub>2</sub> in endosomes, which might be achieved using lipidated antagonists (7) or endosomally targeted nanoparticles (8), could restrict endosomal signaling and ameliorate IBD and other inflammatory and painful diseases associated with enhanced proteolysis and PAR<sub>2</sub> activation.

## Materials and Methods

See *SI Appendix* for details.

**Animals.** The institutional animal care and use committees of New York University and Monash University approved studies of mice.

**Par<sub>2</sub>-muGFP Mice.** A segment of genomic DNA containing exon 2 of mouse *Par<sub>2</sub>* (*F2rl1*) was subcloned from a genomic bacterial artificial chromosome (BAC). The *Par<sub>2</sub>-muGFP* gene was synthesized by fusing muGFP to the 3' end of exon 2. The targeting construct comprised *Par<sub>2</sub>-muGFP*, a phosphoglycerine kinase neomycin cassette flanked by loxP sites. The targeting vector was electroporated into C57BL/6J embryonic stem cells. Clones were screened by Southern blotting, sequenced, and injected into mouse blastocysts. Chimeras were bred with wild-type female mice to generate black F1 progeny. Expression of *Par<sub>2</sub>-muGFP* was confirmed by Southern blotting and PCR.

**qRT-PCR.** cDNA was amplified with primers shown in *SI Appendix, Table S1*.

**Immunofluorescence.** PAR<sub>2</sub>-muGFP was localized using a GFP antibody. Endosomes were detected using EEA1 and Rab7a antibodies, and the plasma membrane was identified using E-cadherin antibodies. Neurons were identified using antibodies to NeuN or PGP9.5.

**RNAscope In Situ Hybridization.** Probes to *F2rl1*, *Gfp*, and *Dnm* isoforms were used for in situ hybridization (*SI Appendix, Table S1*).

**Ex Vivo PAR<sub>2</sub> Trafficking.** Colon segments were incubated with trypsin, 2F, or vehicle. PAR<sub>2</sub>-muGFP was detected by GFP immunofluorescence.

**Colitis-Induced PAR<sub>2</sub> Trafficking.** Mice were treated with DSS or TNBS to evoke colitis.

**Nociception.** Investigators were blinded to treatments and genotypes. PAR<sub>2</sub> agonists were administered into the colon or paw. Abdominal or paw withdrawal thresholds von Frey filaments were assessed.



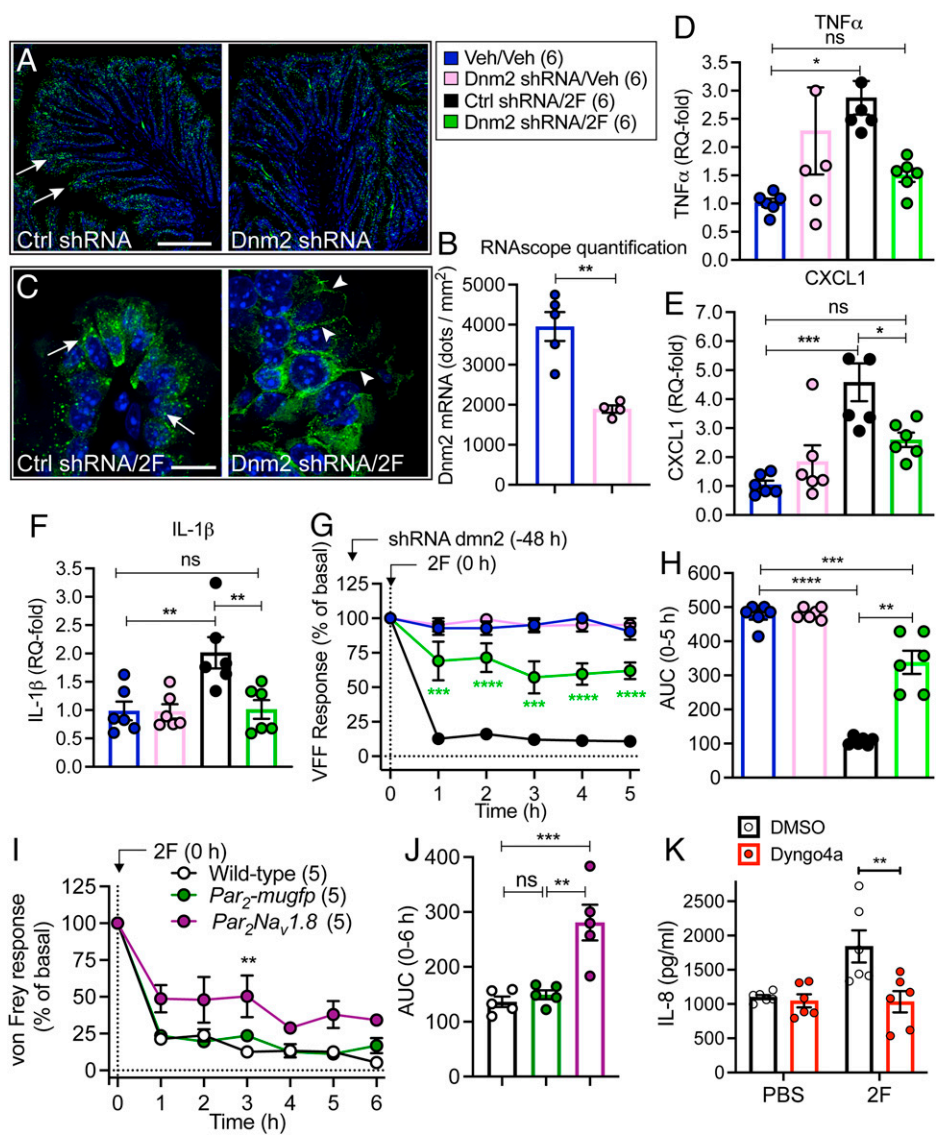


**Fig. 8.** Contribution of Dnm2 to PAR<sub>2</sub>-evoked inflammation and pain in the colon. (A–H) Dnm2 or control (Ctrl) shRNA was administered to *Par<sub>2</sub>-mugfp* mice by intracolonic injection. Mice were studied after 48 h. (A) Localization of *Dnm2* by RNAScope. Representative images are shown. (Scale bars, 100  $\mu$ m.) (B) Quantification of *Dnm2* in the colon. (C) Localization of GFP immunoreactivity in the colon at 5 h after intracolonic injection of 2F. Arrows denote endosomes; arrowheads denote cell surface. (Scale bars, 10  $\mu$ m.) (A–C)  $n = 5$  mice. (D–F) Levels of TNF $\alpha$  (D), CXCL1 (E), and IL-1 $\beta$  (F) in the colon 5 h after intracolonic injection of 2F. (G and H) Abdominal von Frey filament withdrawal responses 1–5 h after intracolonic injection of 2F. (G) Time course. (H) Area under the curve (AUC) from 0 to 5 h. (D–H)  $n = 6$  mice. (I and J) Abdominal von Frey filament withdrawal responses of wild-type, *Par<sub>2</sub>-mugfp*, and *Par<sub>2</sub>Na<sub>v</sub>1.8* mice 1–6 h after intracolonic injection of 2F. (I) Time course. (J) Area under curve from 0 to 6 h.  $n = 5$  mice. (K) Effects of 2F (10  $\mu$ M) on IL-8 release from explants of human colonic mucosa. Explants were preincubated with dynogo4a or vehicle (DMSO, control). Mean  $\pm$  SEM;  $n = 6$ . (B)  $**P < 0.01$  by Student's  $t$  test. (D–J)  $*P < 0.05$ ,  $**P < 0.01$ ,  $***P < 0.001$ , and  $****P < 0.0001$  by one- and two-way ANOVA or Tukey's  $t$  test. (K)  $**P < 0.01$  by Student's  $t$  test.

**In Vivo shRNA Dnm2 Knockdown.** Dnm2shRNA or control shRNA was administered into the colon. PAR<sub>2</sub> endocytosis, expression of cytokines and chemokines, and nociception were studied.

**Cell Lines, cDNA, and Transfection.** Complementary DNA (cDNA) encoding BRET biosensors for PAR<sub>2</sub>, mG $\alpha$ ,  $\beta$ ARR1/2, markers of the plasma membrane, endosomes, and the Golgi apparatus were transfected into T84 cells using Lipofectamine 3000 and into HEK293T cells using PEI. Dominant-negative DnmK44A or Dnm2 or control siRNA (SI Appendix, Table S1) was similarly transfected.

**PAR<sub>2</sub>-muGFP Signaling.** KNRK cells expressing PAR<sub>2</sub>-muGFP or PAR<sub>2</sub>-HA11 were stimulated with PAR<sub>2</sub> agonists, and IP-1 formation was measured.

**PAR<sub>2</sub>-muGFP Signaling.** HEK293T cells expressing PAR<sub>2</sub>-muGFP and CellLight organelle markers were challenged with PAR<sub>2</sub> agonists and examined by confocal microscopy.

**Trafficking of PAR<sub>2</sub>,  $\beta$ ARR, and G $\alpha_q$ .** HEK293T cells stably expressing FLAG-PAR<sub>2</sub>-HA were transfected with YFP- $\beta$ ARR1 plus YFP- $\beta$ ARR2. Cells were challenged with PAR<sub>2</sub> agonists, and then PAR<sub>2</sub>, G $\alpha_q$ , and EEA1 were localized by immunofluorescence and confocal microscopy.

**BRET Assays.** T84 or HEK293T cells were preincubated with luciferase substrates and challenged with PAR<sub>2</sub> agonists, and BRET was measured using a luminometer.

**T84 TEER.** T84 cells were cultured on Transwell inserts until TEER was  $>2,000 \Omega$ . PAR<sub>2</sub> agonists were added to the basolateral compartment, and TEER was measured at 0 and 6 h. GB88 or vehicle was added to the basolateral and apical compartments 30 min before PAR<sub>2</sub> agonists. Dnm2 siRNA or control siRNA and Lipofectamine 3000 were added to both compartments overnight before PAR<sub>2</sub> agonists.

**IL-8 Secretion from Human Colonic Mucosa.** Institutional review board approval was waived since no patient-identifiable information was obtained. IL-8 secretion was measured by enzyme-linked immunosorbent assay (ELISA) from isolated segments of colonic mucosa collected from patients undergoing resection for treatment of colon cancer.

**Statistics.** Data are presented as mean  $\pm$  SEM. Differences were assessed using Student's *t* test for two comparisons and one- or two-way ANOVA and Tukey's, Dunnett's, or Sidak's post hoc test for multiple comparisons. *P* < 0.05 was considered significant at the 95% confidence level.

1. M. Canals, D. P. Poole, N. A. Veldhuis, B. L. Schmidt, N. W. Bunnett, G-protein-coupled receptors are dynamic regulators of digestion and targets for digestive diseases. *Gastroenterology* **156**, 1600–1616 (2019).
2. Y. K. Peterson, L. M. Luttrell, The diverse roles of arrestin scaffolds in G protein-coupled receptor signaling. *Pharmacol. Rev.* **69**, 256–297 (2017).
3. K. A. DeFea *et al.*, Beta-arrestin-dependent endocytosis of proteinase-activated receptor 2 is required for intracellular targeting of activated ERK1/2. *J. Cell Biol.* **148**, 1267–1281 (2000).
4. R. Irannejad *et al.*, Conformational biosensors reveal GPCR signalling from endosomes. *Nature* **495**, 534–538 (2013).
5. D. D. Jensen *et al.*, Neurokinin 1 receptor signaling in endosomes mediates sustained nociception and is a viable therapeutic target for prolonged pain relief. *Sci. Transl. Med.* **9**, eaa13447 (2017).
6. N. N. Jimenez-Vargas *et al.*, Endosomal signaling of delta opioid receptors is an endogenous mechanism and therapeutic target for relief from inflammatory pain. *Proc. Natl. Acad. Sci. U.S.A.* **117**, 15281–15292 (2020).
7. N. N. Jimenez-Vargas *et al.*, Protease-activated receptor-2 in endosomes signals persistent pain of irritable bowel syndrome. *Proc. Natl. Acad. Sci. U.S.A.* **115**, E7438–E7447 (2018).
8. P. D. Ramirez-Garcia *et al.*, A pH-responsive nanoparticle targets the neurokinin 1 receptor in endosomes to prevent chronic pain. *Nat. Nanotechnol.* **14**, 1150–1159 (2019).
9. R. E. Yarwood *et al.*, Endosomal signaling of the receptor for calcitonin gene-related peptide mediates pain transmission. *Proc. Natl. Acad. Sci. U.S.A.* **114**, 12309–12314 (2017).
10. A. Godbole, S. Lyga, M. J. Lohse, D. Calebiro, Internalized TSH receptors en route to the TGN induce local G<sub>γ</sub>-protein signaling and gene transcription. *Nat. Commun.* **8**, 1–15 (2017).
11. M. Stoerber *et al.*, A genetically encoded biosensor reveals location bias of opioid drug action. *Neuron* **98**, 963–976 (2018).
12. V. S. Ossovskaya, N. W. Bunnett, Protease-activated receptors: Contribution to physiology and disease. *Physiol. Rev.* **84**, 579–621 (2004).
13. S. K. Bohm *et al.*, Molecular cloning, expression and potential functions of the human proteinase-activated receptor-2. *Biochem. J.* **314**, 1009–1016 (1996).
14. C. U. Corvera *et al.*, Mast cell tryptase regulates rat colonic myocytes through proteinase-activated receptor 2. *J. Clin. Invest.* **100**, 1383–1393 (1997).
15. E. Camerer, W. Huang, S. R. Coughlin, Tissue factor- and factor X-dependent activation of protease-activated receptor 2 by factor VIIa. *Proc. Natl. Acad. Sci. U.S.A.* **97**, 5255–5260 (2000).
16. K. Oikonomopoulou *et al.*, Proteinase-activated receptors, targets for kallikrein signaling. *J. Biol. Chem.* **281**, 32095–32112 (2006).
17. N. H. Tu *et al.*, Legumain induces oral cancer pain by biased agonism of protease-activated receptor-2. *J. Neurosci.* **41**, 193–210 (2021).
18. P. Zhao *et al.*, Cathepsin S causes inflammatory pain via biased agonism of PAR2 and TRPV4. *J. Biol. Chem.* **289**, 27215–27234 (2014).
19. P. Zhao *et al.*, Neutrophil elastase activates protease-activated receptor-2 (PAR2) and transient receptor potential vanilloid 4 (TRPV4) to cause inflammation and pain. *J. Biol. Chem.* **290**, 13875–13887 (2015).
20. B. M. Anderson *et al.*, Application of a chemical probe to detect neutrophil elastase activation during inflammatory bowel disease. *Sci. Rep.* **9**, 13295 (2019).
21. N. Barlow *et al.*, Demonstration of elevated levels of active cathepsin S in dextran sulfate sodium colitis using a new activatable probe. *Neurogastroenterol. Motil.* **27**, 1675–1680 (2015).
22. F. Cattaruzza *et al.*, Cathepsin S is activated during colitis and causes visceral hyperalgesia by a PAR2-dependent mechanism in mice. *Gastroenterology* **141**, 1864–1874 (2011).

**Data Availability.** All study data are included in the article and/or [SI Appendix](#).

**ACKNOWLEDGMENTS.** This study was supported by grants from the NIH (NS102722, DE026806, DK118971, and DE029951 to N.W.B. and B.L.S.), Department of Defense (W81XWH1810431 to N.W.B. and B.L.S.), National Health and Medical Research Council (63303 to N.W.B.), and Australian Research Council Centre of Excellence in Convergent Bio-Nano Science and Technology (N.W.B.). We thank S. O'Brien (University of Birmingham) for guidance with the nbBRET assay. Cartoons were made with BioRender.

23. G. S. Cottrell *et al.*, Protease-activated receptor 2, dipeptidyl peptidase I, and proteases mediate Clostridium difficile toxin A enteritis. *Gastroenterology* **132**, 2422–2437 (2007).
24. A. Denadai-Souza *et al.*, Functional proteomic profiling of secreted serine proteases in health and inflammatory bowel disease. *Sci. Rep.* **8**, 7834 (2018).
25. K. K. Hansen *et al.*, A major role for proteolytic activity and proteinase-activated receptor-2 in the pathogenesis of infectious colitis. *Proc. Natl. Acad. Sci. U.S.A.* **102**, 8363–8368 (2005).
26. C. Jacob *et al.*, Mast cell tryptase controls paracellular permeability of the intestine. Role of protease-activated receptor 2 and beta-arrestins. *J. Biol. Chem.* **280**, 31936–31948 (2005).
27. W. Kong *et al.*, Luminal trypsin may regulate enterocytes through proteinase-activated receptor 2. *Proc. Natl. Acad. Sci. U.S.A.* **94**, 8884–8889 (1997).
28. M. Steinhoff *et al.*, Agonists of proteinase-activated receptor 2 induce inflammation by a neurogenic mechanism. *Nat. Med.* **6**, 151–158 (2000).
29. N. Vergnolle *et al.*, Proteinase-activated receptor-2 and hyperalgesia: a novel pain pathway. *Nat. Med.* **7**, 821–826 (2001).
30. N. Cenac *et al.*, Proteinase-activated receptor-2-induced colonic inflammation in mice: Possible involvement of afferent neurons, nitric oxide, and paracellular permeability. *J. Immunol.* **170**, 4296–4300 (2003).
31. D. J. Scott *et al.*, A novel ultra-stable, monomeric green fluorescent protein for direct volumetric imaging of whole organs using CLARITY. *Sci. Rep.* **8**, 667 (2018).
32. A. R. B. Thomsen, D. D. Jensen, G. A. Hicks, N. W. Bunnett, Therapeutic targeting of endosomal G-protein-coupled receptors. *Trends Pharmacol. Sci.* **39**, 879–891 (2018).
33. C. Jacob *et al.*, c-Cbl mediates ubiquitination, degradation, and down-regulation of human protease-activated receptor 2. *J. Biol. Chem.* **280**, 16076–16087 (2005).
34. D. D. Jensen *et al.*, Protein kinase D and G $\beta\gamma$  subunits mediate agonist-evoked translocation of Protease-activated Receptor-2 from the Golgi apparatus to the plasma membrane. *J. Biol. Chem.* **291**, 11285–11299 (2016).
35. P. Zhao *et al.*, Protein kinase D and G $\beta\gamma$  mediate sustained nociceptive signaling by biased agonists of Protease-Activated Receptor-2. *J. Biol. Chem.* **294**, 10649–10662 (2019).
36. A. H. Nguyen *et al.*, Structure of an endosomal signaling GPCR-G protein- $\beta$ -arrestin megacomplex. *Nat. Struct. Mol. Biol.* **26**, 1123–1131 (2019).
37. A. R. B. Thomsen *et al.*, GPCR-G protein- $\beta$ -arrestin super-complex mediates sustained G protein signaling. *Cell* **166**, 907–919 (2016).
38. A. S. Dixon *et al.*, NanoLuc complementation reporter optimized for accurate measurement of protein interactions in cells. *ACS Chem. Biol.* **11**, 400–408 (2016).
39. N. Cenac *et al.*, Induction of intestinal inflammation in mouse by activation of proteinase-activated receptor-2. *Am. J. Pathol.* **161**, 1903–1915 (2002).
40. D. D. Jensen *et al.*, Endothelin-converting enzyme 1 and  $\beta$ -arrestins exert spatiotemporal control of substance P-induced inflammatory signals. *J. Biol. Chem.* **289**, 20283–20294 (2014).
41. D. P. Poole *et al.*, Localization and regulation of fluorescently labeled delta opioid receptor, expressed in enteric neurons of mice. *Gastroenterology* **141**, 982–991 (2011).
42. G. Scherrer *et al.*, Knockin mice expressing fluorescent delta-opioid receptors uncover G protein-coupled receptor dynamics in vivo. *Proc. Natl. Acad. Sci. U.S.A.* **103**, 9691–9696 (2006).
43. N. Cenac *et al.*, PAR2 activation alters colonic paracellular permeability in mice via IFN-gamma-dependent and -independent pathways. *J. Physiol.* **558**, 913–925 (2004).
44. S. N. Hassler *et al.*, The cellular basis of protease-activated receptor 2-evoked mechanical and affective pain. *JCI Insight* **5**, e12793 (2020).
45. G. S. Cottrell, S. Amadesi, E. F. Grady, N. W. Bunnett, Trypsin IV, a novel agonist of protease-activated receptors 2 and 4. *J. Biol. Chem.* **279**, 13532–13539 (2004).
46. A. Caminero *et al.*, Duodenal bacterial proteolytic activity determines sensitivity to dietary antigen through protease-activated receptor-2. *Nat. Commun.* **10**, 1–14 (2019).